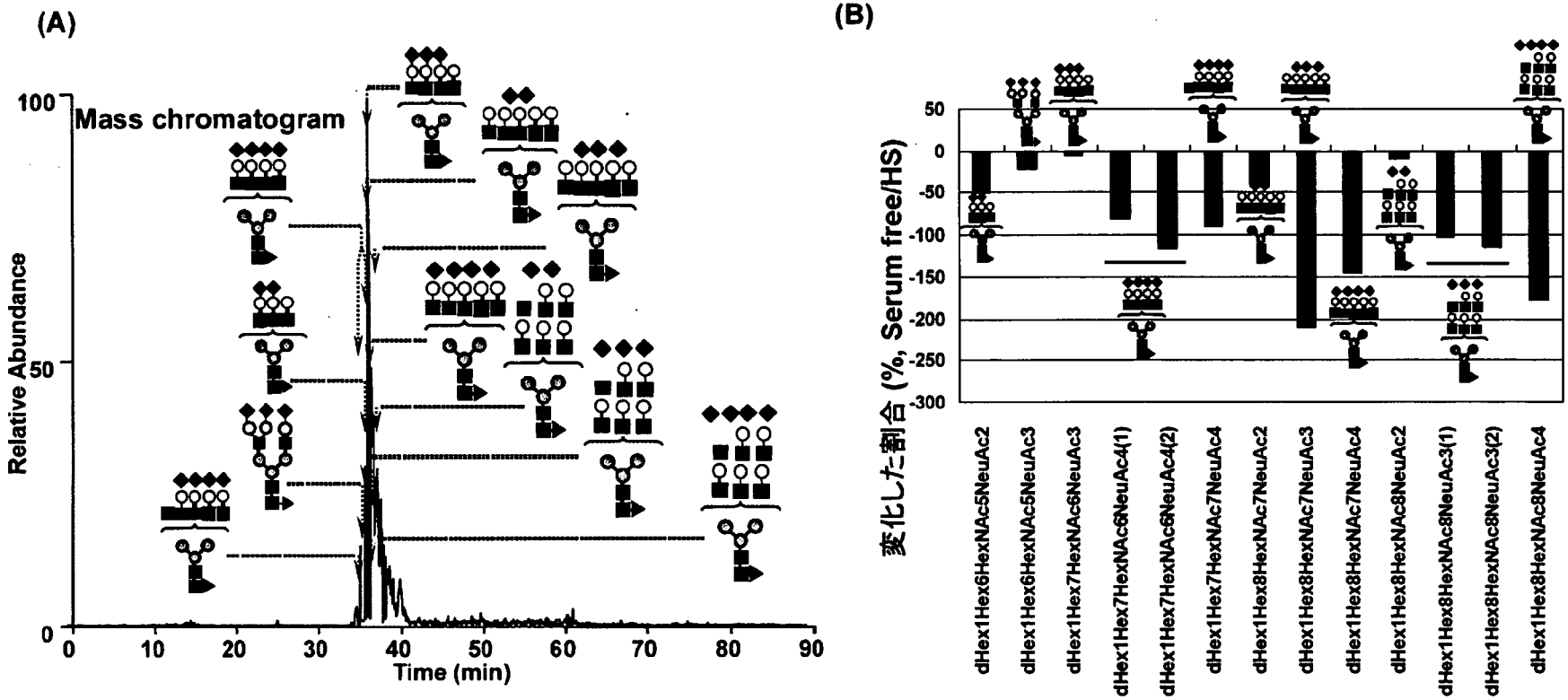

Fig.68　3及び4本鎖糖鎖の比較定量解析　(serum free vs HS)

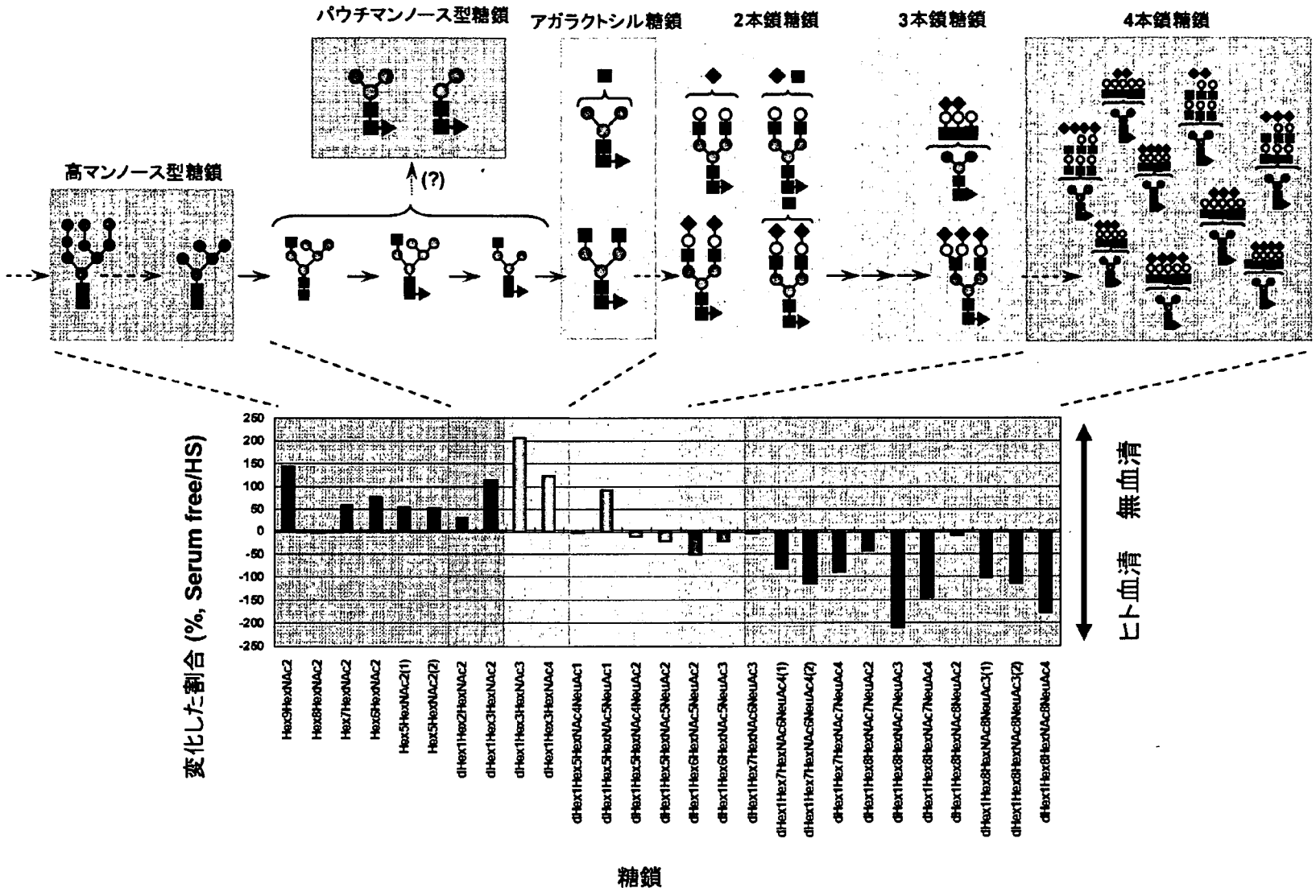

Fig.69 N結合型糖鎖生合成経路と無血清培地及び HS 添加培地で培養したHL60RG膜画分由来糖鎖の比較定量解析

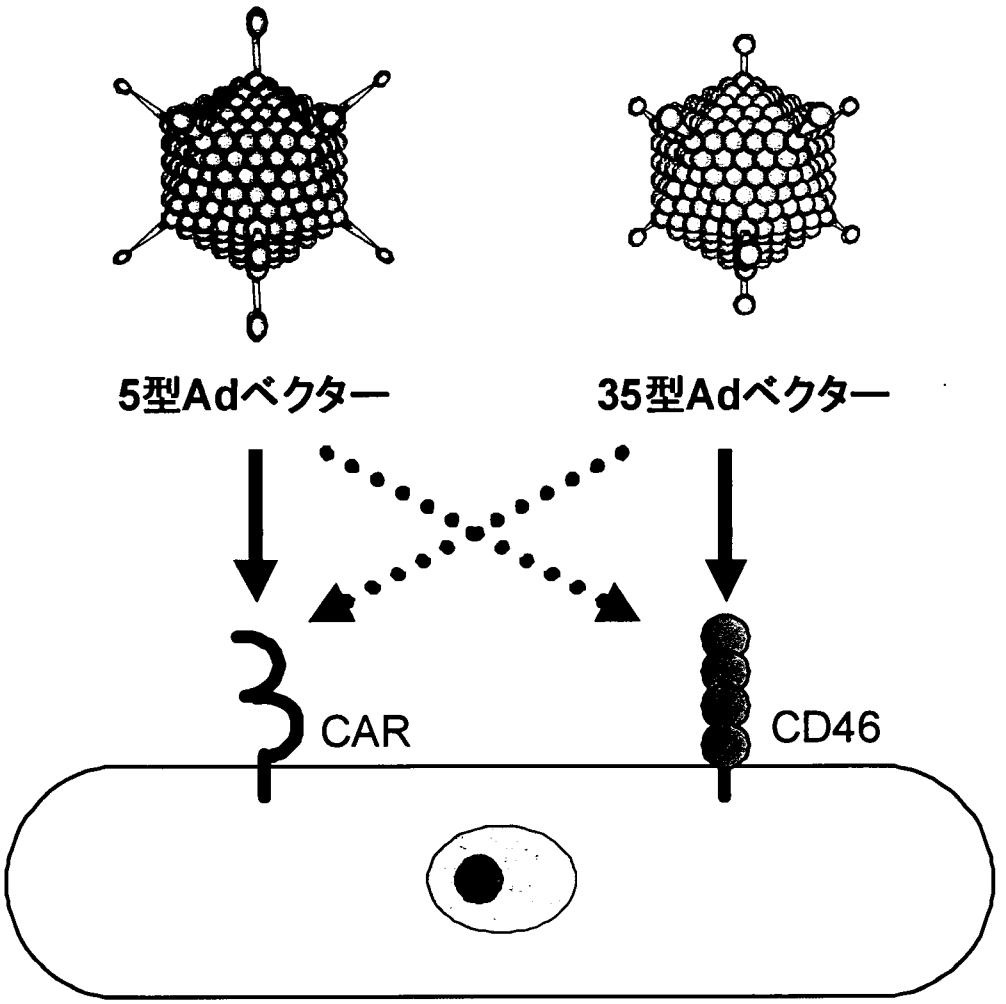

Fig.70 **Diagram of interaction between Ad vectors and receptors.** Ad serotype 5 vectors (subgroup C) recognize coxsakievirus and adenovirus receptor (CAR), in contrast, Ad serotype 35 vectors (subgroup B) utilized human CD46 for infection.

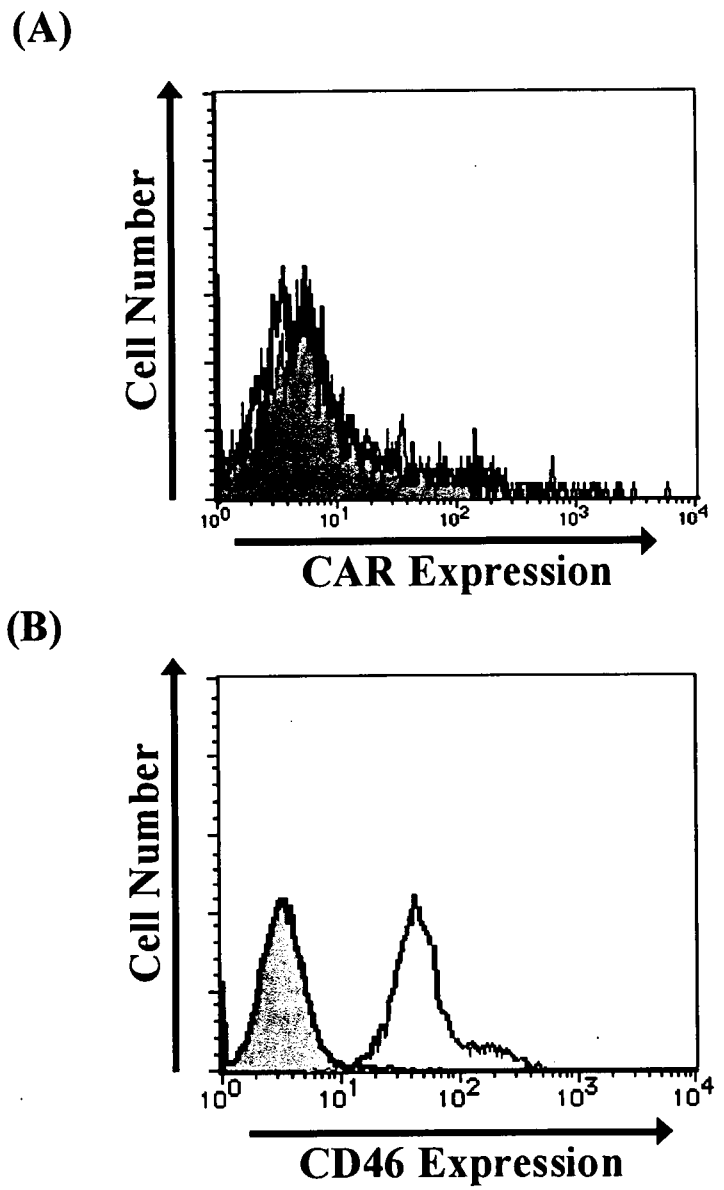

Fig.71 **Expression of Ad receptors on human bone-marrow CD34$^+$ cells.** (A) coxsachievirus and adenovirus receptor (CAR) (a receptor for Ad5), (B) CD46 (a receptor for Ad35). The cells were incubated with FITC-conjugated anti-CD46 antibody for measurement of CD46. For analysis of CAR expression, the cells were treated anti-CAR antibody. After a 1-hr incubation, cells were washed and resuspended in a staining buffer containing phycoerythrin (PE)-labeled anti-mouse IgG antibody. After a 1-hr incubation, the cells were subjected to flowcytomteric analysis. As a negative control, the cells were incubated with an irrelevant antibody (shaded histogram).

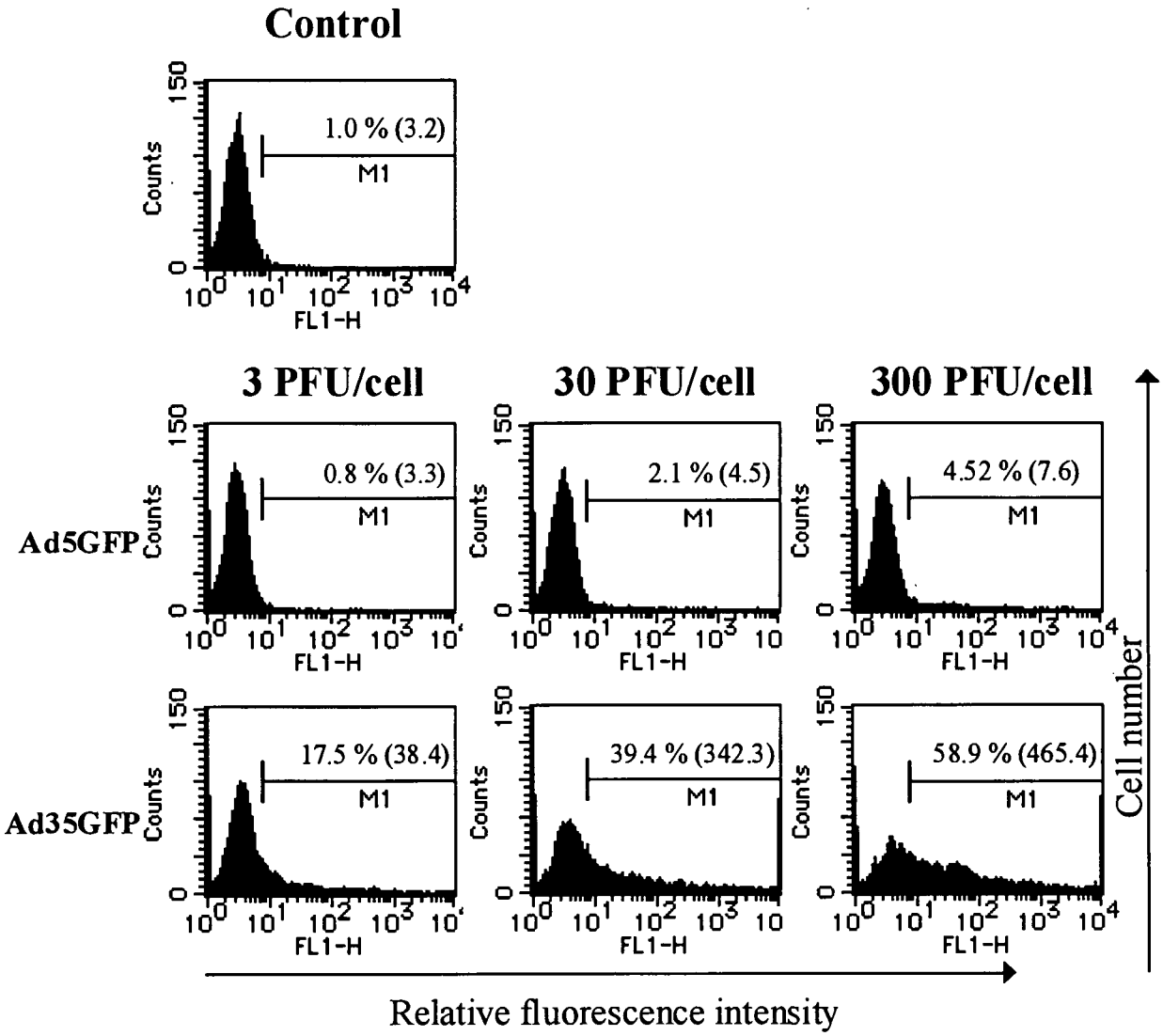

Fig.72 **GFP expression in human CD34$^+$ cells transduced with Ad5GFP and Ad35GFP.** Human CD34$^+$ cells were suspended in the medium containing the cytokine cocktail (3 x 10^5 cells/ml). The cells were seeded into a 96-well plate (1 x 10^4 cells/well), and equal volumes of the Ad vectors were applied to the cells 16-18 hrs after seeding. Forty-eight hour later, GFP expression in the cells were measured by flow cytometry.

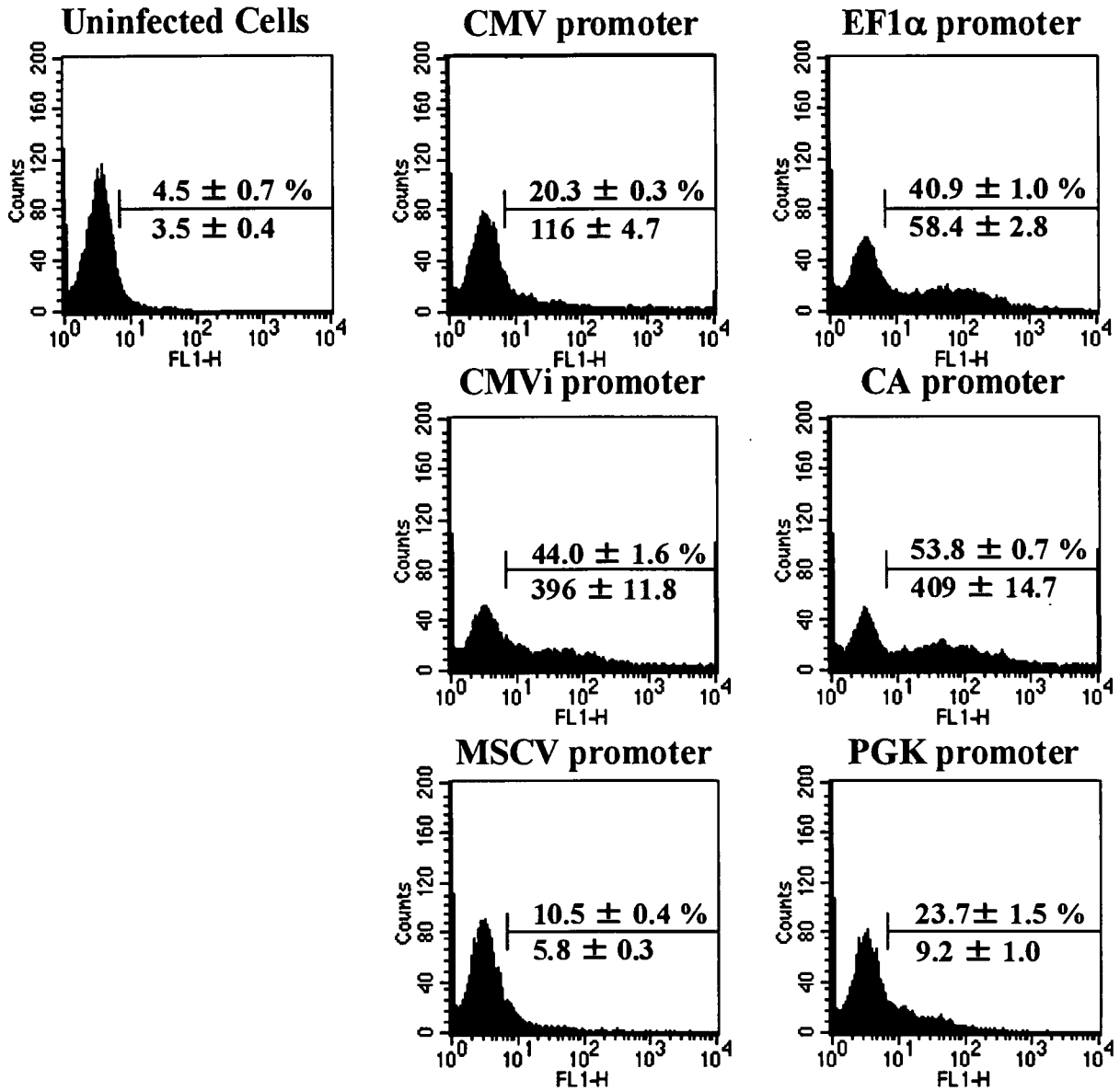

Fig.73 Comparison of promoter activities in human bone marrow CD34⁺ cells transduced with Ad35 vectors. The results are shown as a percentage of GFP-positive cells (upper) and the mean fluorescence intensity (MFI) (lower) in the panel. The CD34⁺ cells were transduced with Ad35 vectors at 6000 VP/cell for 6 hrs, washed, and resuspended in medium. Forty-eight hours later, GFP expression was measured by flow cytometry. All data represent the means ± S.D. of three experiments.

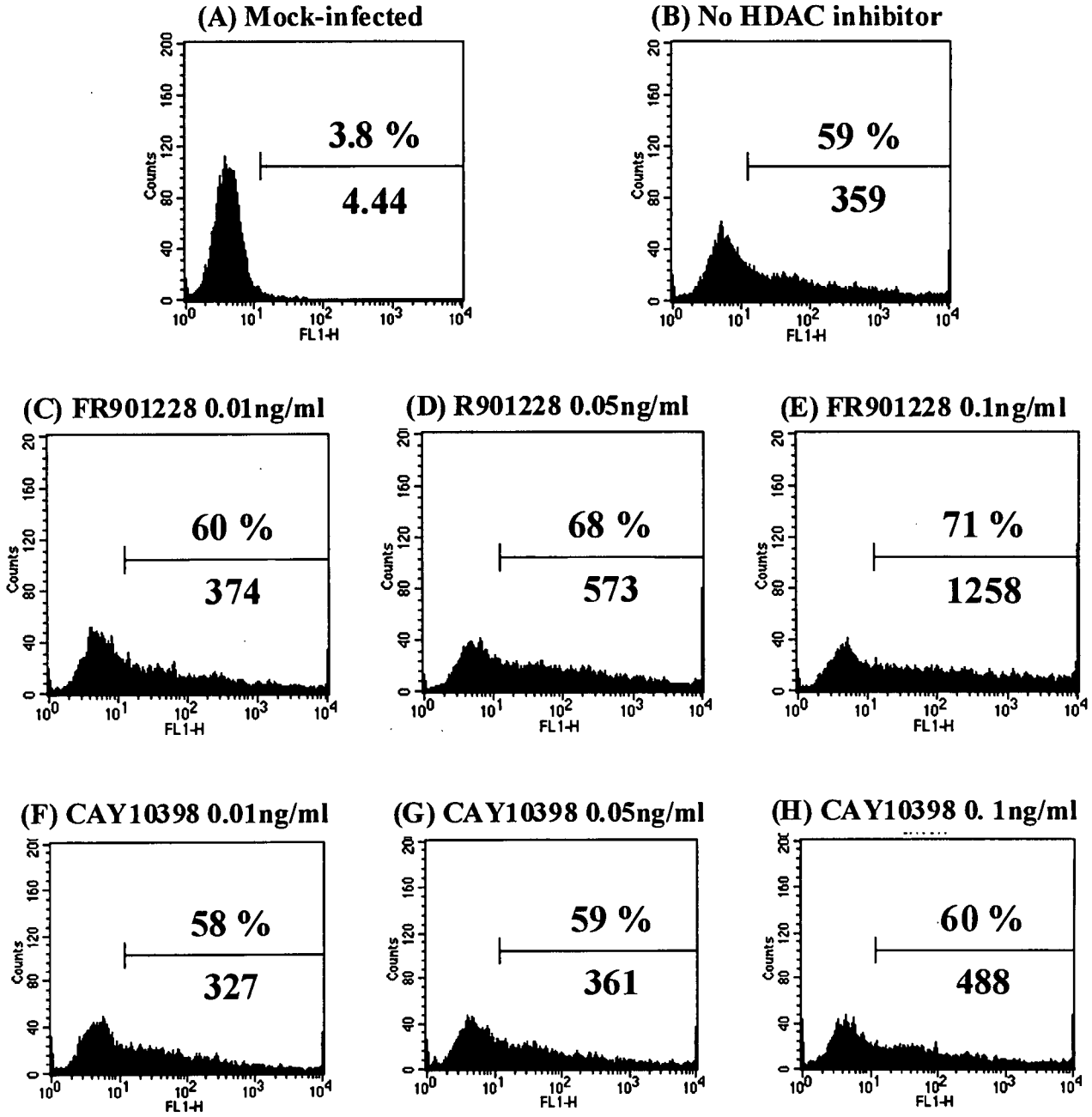

Fig.74 Effect of treatment with HDAC inhibitors on the transduction of human bone-marrow CD34$^+$ cells. The results are shown as a percentage of GFP-positive cells (upper) and the mean fluorescence intensity (MFI) (lower) in the panel. The CD34$^+$ cells were incubated with HDAC inhibitors at the indicated concentrations and Ad35 vectors at 6000 VP/cell for 6 hrs, washed, and resuspended in medium. Forty-eight hours later, GFP expression was measured by flow cytometry.

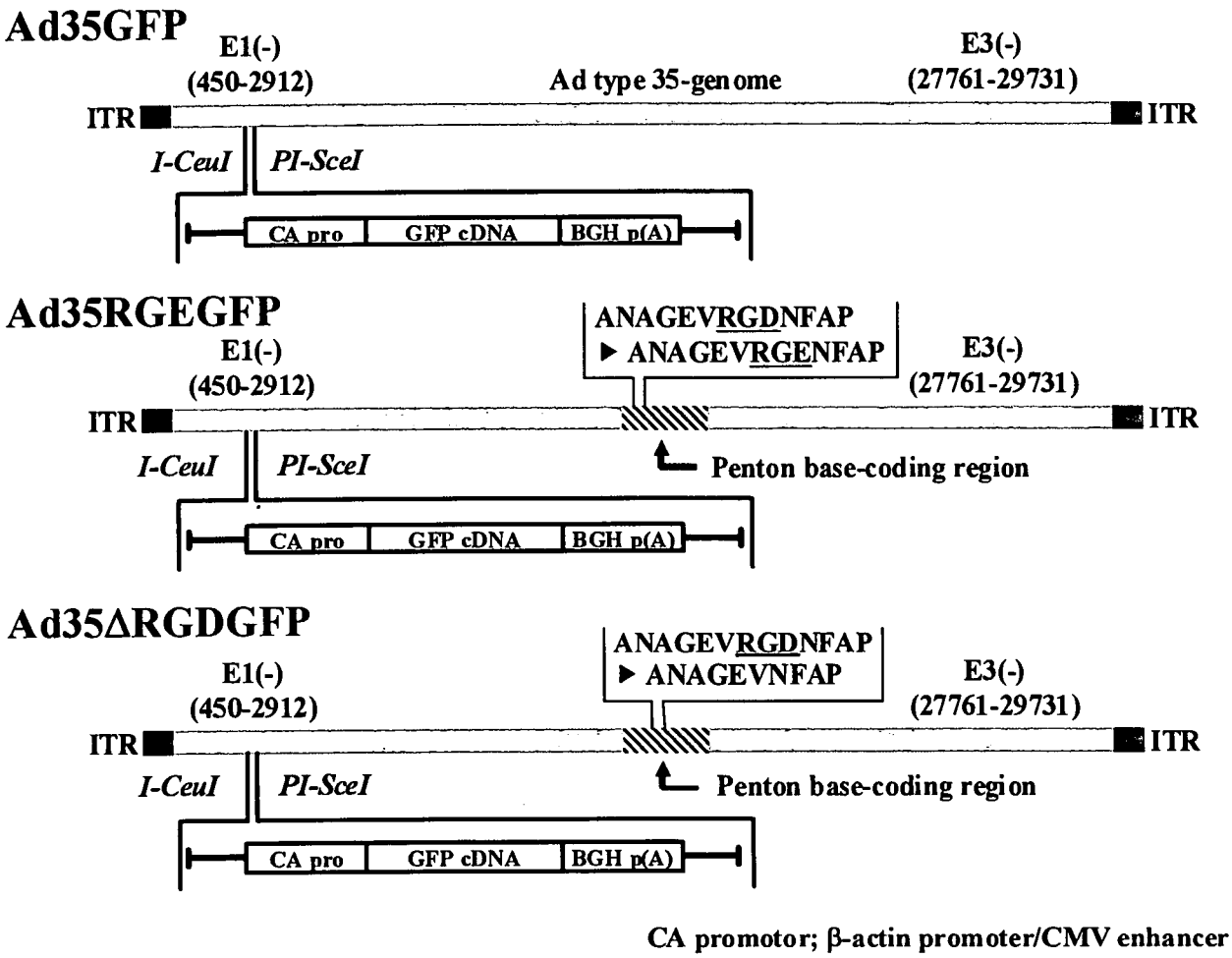

Fig.75 Schematic representation of adenovirus used in this study

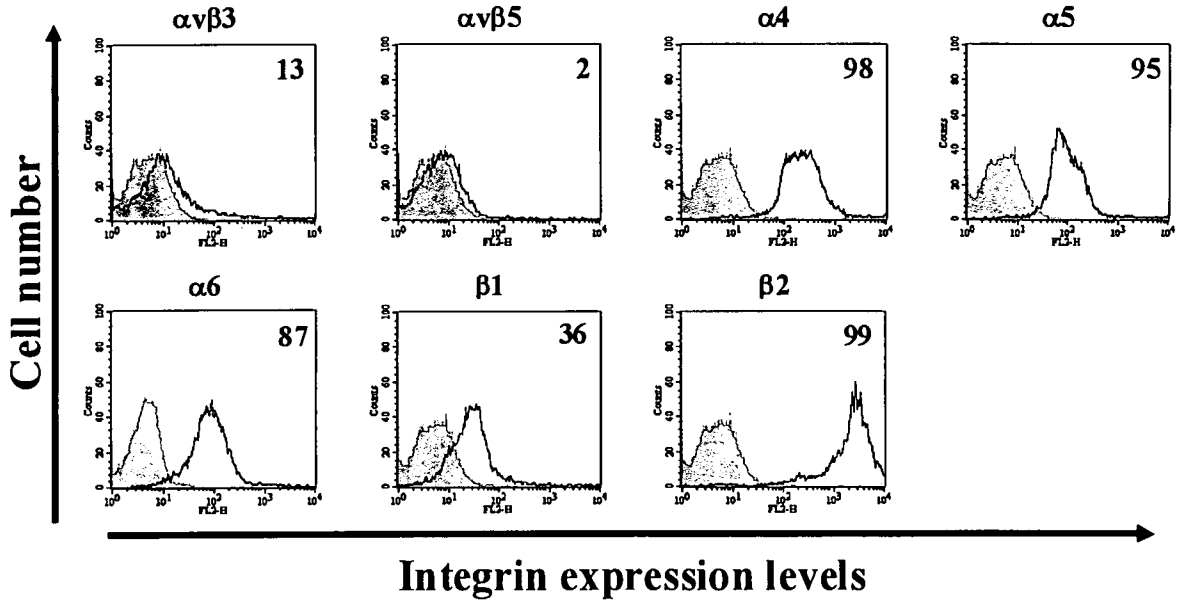

Fig.76 Flow cytometric profiles of integrin expression on human bone marrow-derived CD34$^+$ cells. The cells were stained with anti-integrin antibodies, followed by a PE-labeled secondary antibody, and subsequently analyzed by a flow cytometer (thick line). As a negative control, the cells were incubated with isotype control antibody (shaded histogram). Percentage of positive cells is showed by number in upper right-hand corner of each profile.

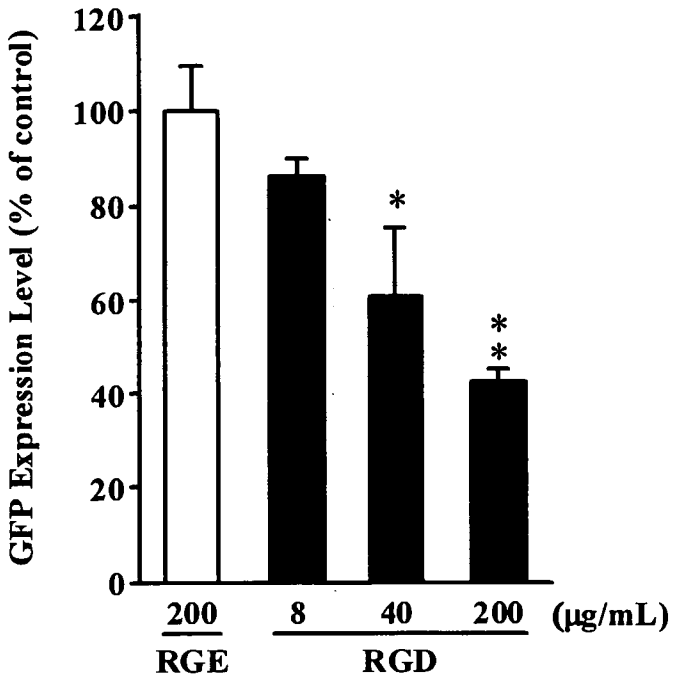

Fig.77 Inhibition of Ad35 vector-mediated transduction by RGD synthetic peptides. Human CD34$^+$ cells were incubated with RGD synthetic peptides at the indicated concentrations at 4 °C for 1 h prior to the addition of Ad35GFP, and then left for 3 h at 37 °C. Samples were then washed, resuspended in a fresh medium, and incubated at 37 °C. GFP expression levels were measured 48 h after transduction by flow cytometry. The data were normalized to the GFP expression levels (MFI) in human CD34$^+$ cells in the presence of control RGE peptides. The data are expressed as the mean ± S.D. (n=3) *$P < 0.05$, **$P < 0.001$ for comparison with the cells pretreated with control RGE peptides.

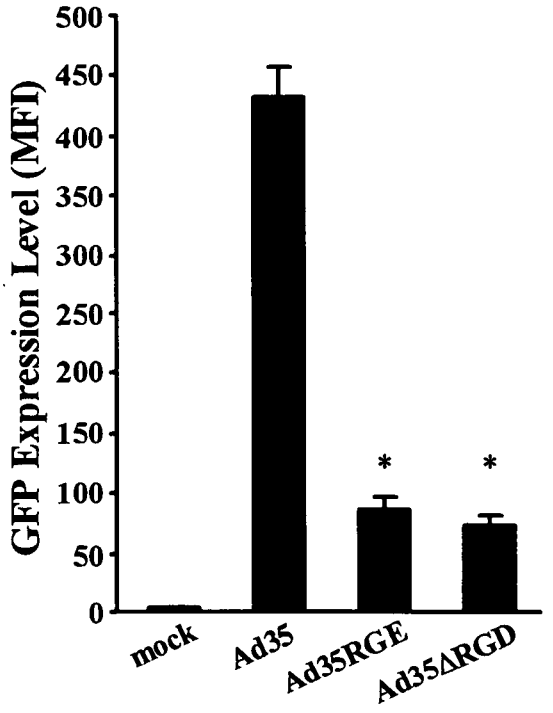

Fig.78 Comparison of GFP expression levels in human CD34⁺ cells transduced with Ad35GFP, Ad35RGEGFP, and Ad35DRGDGFP. Human CD34⁺ cells were transduced with 6000 VP/cell of Ad35GFP, Ad35RGEGFP, and Ad35ΔRGDGFP for 6 h at 37 °C. GFP expression levels (MFI) were measured 48 h after transduction using flow cytometry. The data are expressed as the mean ± S.D. (n=3) *P < 0.001 for comparison with the cells transduced with Ad35GFP.

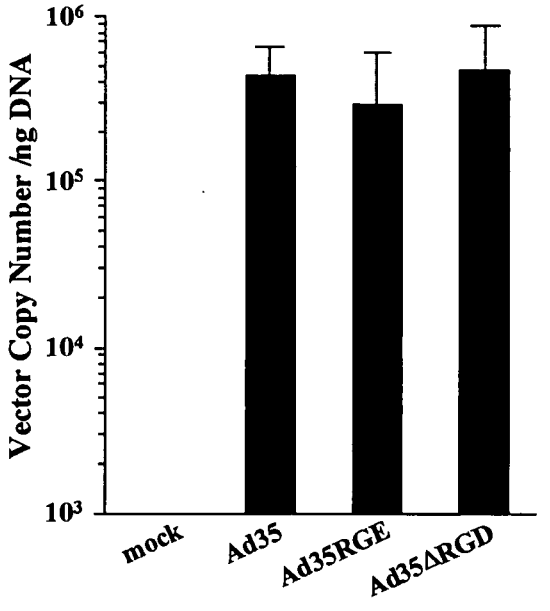

Fig.79 Viral uptake of several Ad35 vectors in human CD34⁺ cells. The cells were transduced with Ad35GFP, Ad35RGEGFP, and Ad35ΔRGDGFP for 3 h at 37 °C. After incubation, the cells were washed five times with ice-cold PBS, and total DNA, including the Ad vector DNA, was extracted. The copy numbers of the Ad vector DNA were quantified by TaqMan PCR. The data are expressed as the mean mean ± S.D. (n=4)

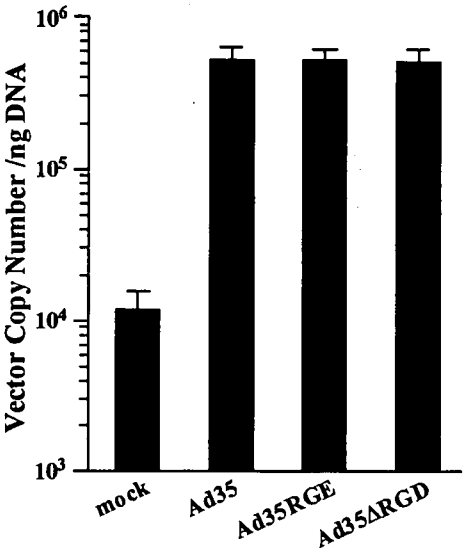

Fig.80 Cellular attachment of Ad35 vectors on human CD34$^+$ cells. Human CD34$^+$ cells were incubated with Ad35GFP, Ad35RGEGFP, and Ad35ΔRGDGFP for 3 h at 4 °C. After incubation, the cells were washed five times with ice-cold PBS, and total DNA, including the Ad vector DNA, was extracted. The copy numbers of the Ad vector DNA were quantified by TaqMan PCR. The data are expressed as the mean mean ± S.D. (n=4)

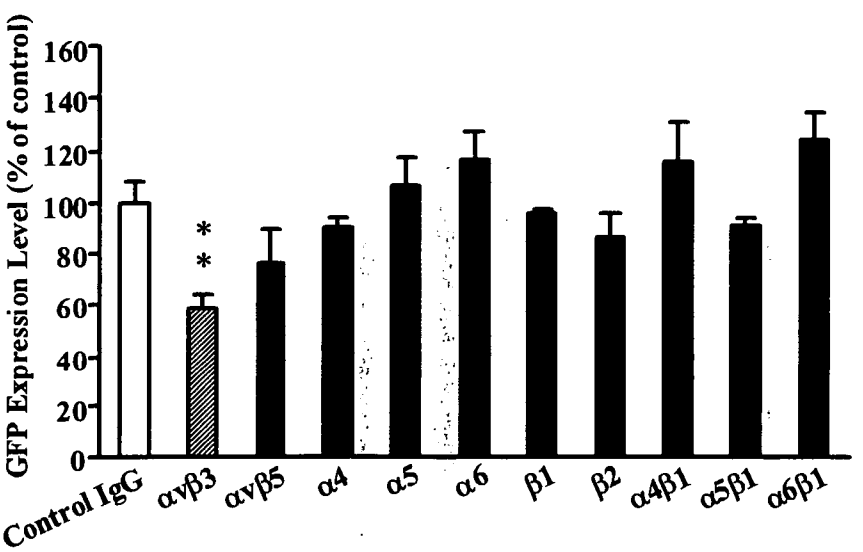

Fig.81 Inhibition of Ad35 vector-mediated transduction by monoclonal anti-integrin antibodies. Human CD34$^+$ cells were preincubated with each antibody at 50 μg/mL for 1 h at 4 °C, and then added 3000 VP/cells of Ad35GFP. The cells were incubated at 3 h at 37 °C, and then cells were washed, and resuspended in a fresh medium and incubated at 37 °C. GFP expression levels were measured 48 h after transduction using flow cytometry. The data were normalized to the GFP expression levels (MFI) in human CD34$^+$ cells in the presence of control mouse IgG. The data are expressed as the mean ± S.D. (n=3) $^*P < 0.05$, $^{**}P < 0.01$ for comparison with the cells preincubated with control IgG.

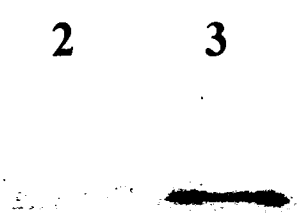

Fig.82 Expression of Bcl-xL and Bcl-FNK following Ad35 vector transduction in human bone-marrow CD34+ cells. Lane 1; mock, lane 2; Ad35-BclxL, lane 3; Ad35-BclFNK, lane 4; Ad35-GFP. The CD34+ cells were transduced with Ad35 vectors at 6000 VP/cell for 6 hr. Following a 48 hr-incubation, the cells were collected and expression of Bcl-xL and Bcl-FNK was asssessed by Western blotting analysis. One representative experiment of three is shown.

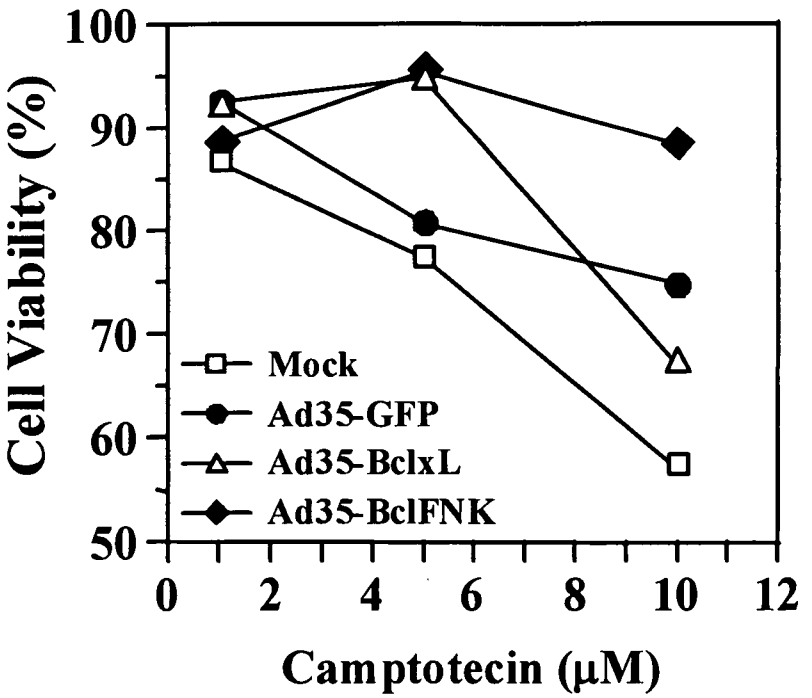

Fig.83 Survival of human bone-marrow CD34+ cells in the presence of Camptotecin. The CD34+ cells were transduced with Ad35 vectors at 6000 VP/cell for 6 hr. Following a 6 day-incubation, Camptotecin was added to the cells at the indicated concentrations, and incubated for 48 hrs. Viability of the cells was assessed by trypan blue exclusion assays. The results shown are mean of two experiments.

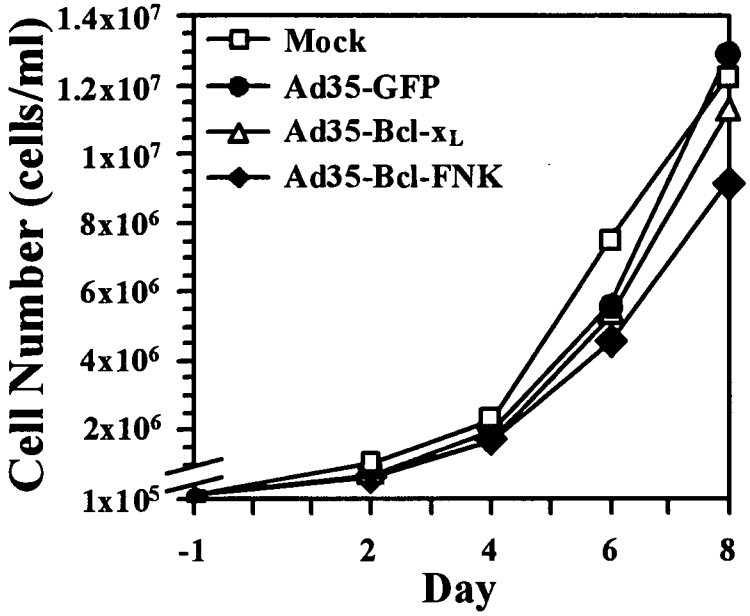

Fig.84 Growth ratio of human bone-marrow CD34+ cells following Ad35 vector Transduction. The CD34+ cells were transduced with Ad35 vectors at 6000 VP/cell for 6 hr. Cell numbers were measured at the indicated time points. The results shown are mean of 2 experiments.

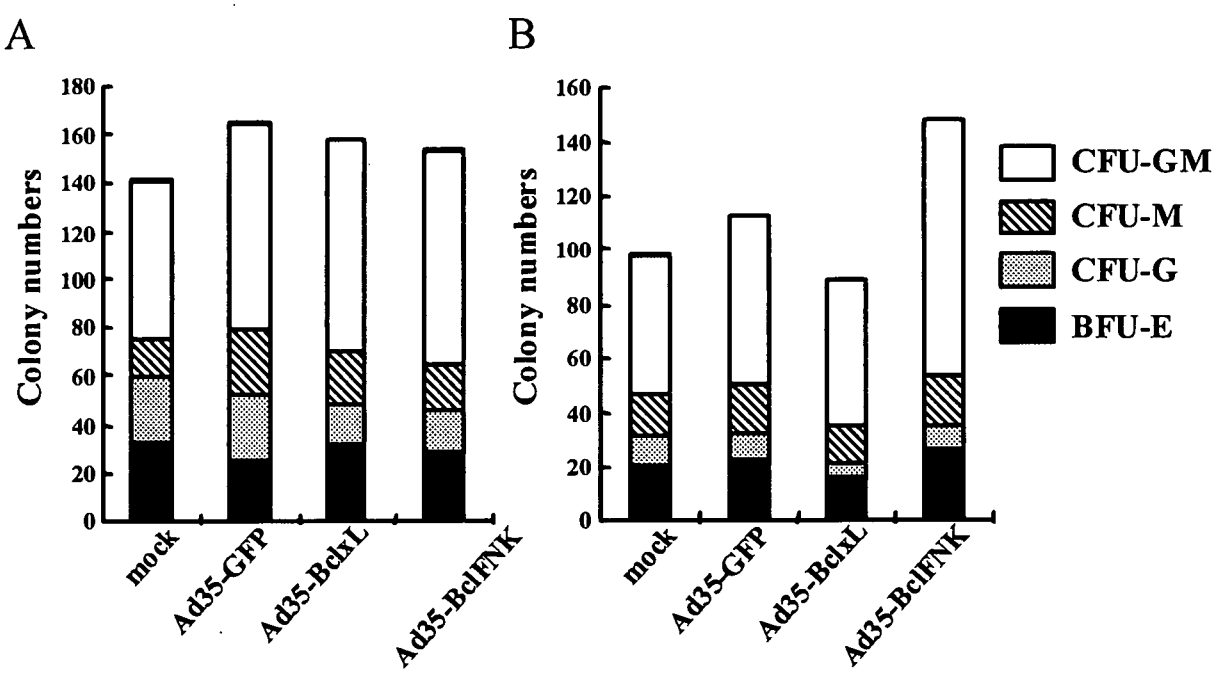

Fig.85 Colony forming assay of human bone-marrow CD34+ cells following Ad35 vector Transduction. The CD34+ cells were transduced with Ad35 vectors at 6000 VP/cell for 6 hr. The cells were collected and subjected to colony forming assay at (A) 2 days or 8 days after transduction. The results shown are the mean of 4 experiments.

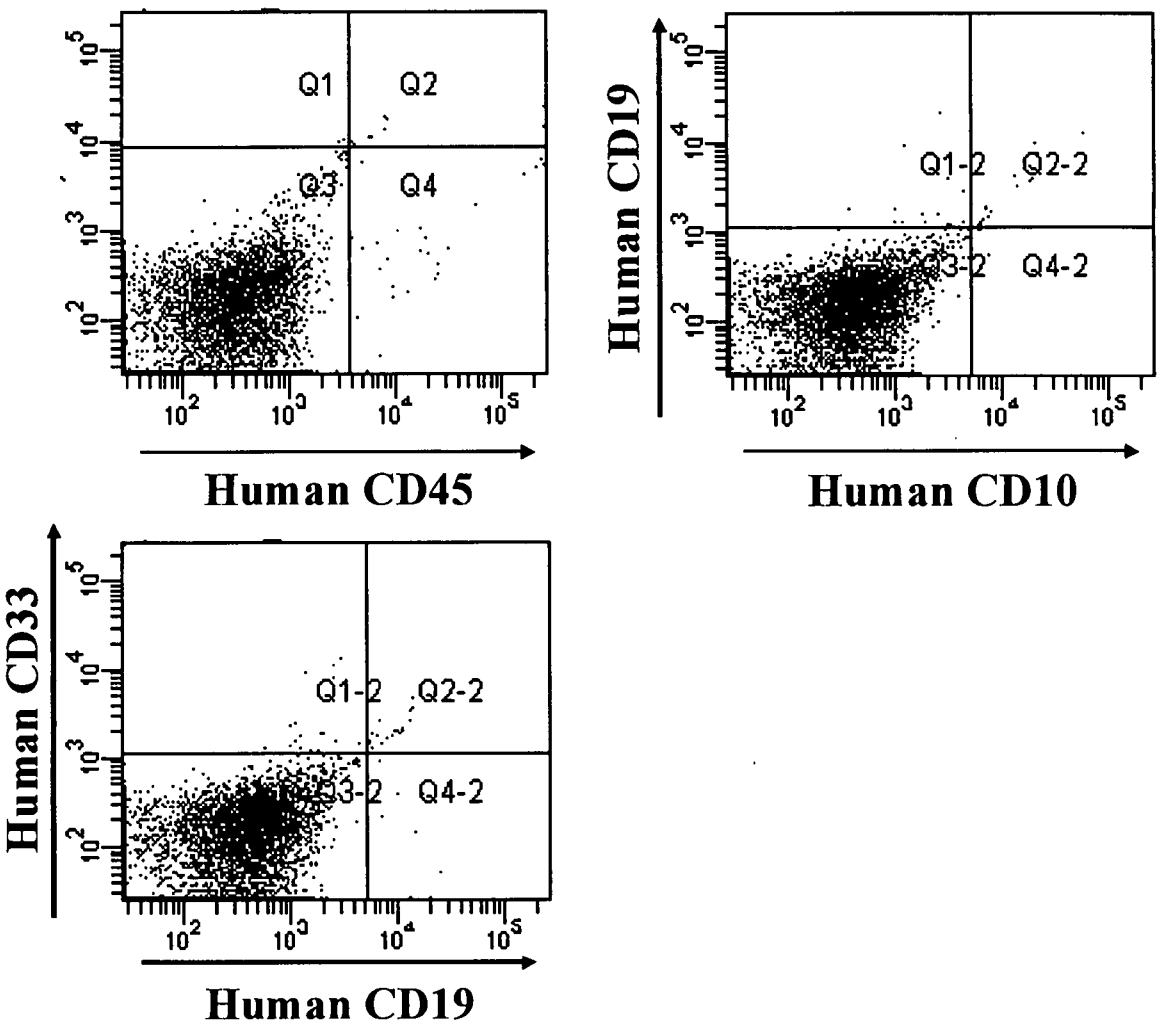

Fig.86 **Analysis of human hematopoietic cells in NOG recipients. The $CD34^+$ cells were transduced with Bcl-FNK-expressing Ad35 vectors at 6000 VP/cell for 6 hr. Following a 48 hr-incubation, $1x10^5$ cells were transplanted into irradiated NOG mice. Bone marrow cells were recovered and analyzed using flowcytometry 20 weeks after transplantation.**

	EPC	OEC
形態	 Spindle shape (or round shape ?)	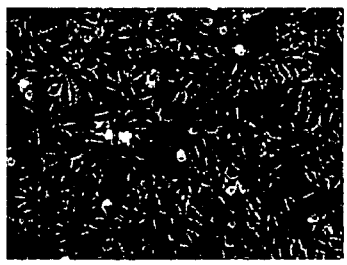 Cobblestone
特徴	細胞のheterogeneity高い 増殖性低い	均質な細胞 増殖性高い
機能	血管形成を促進する サイトカイン等を放出	新生血管に取り込まれる
臨床応用例	あり	なし
有用性確保のための課題	増幅法の確立 特性解析	誘導効率の改善 (現状:1コロニー/10^7MNCs程度) 特性解析

Fig.87 Early EPCとOECの特徴

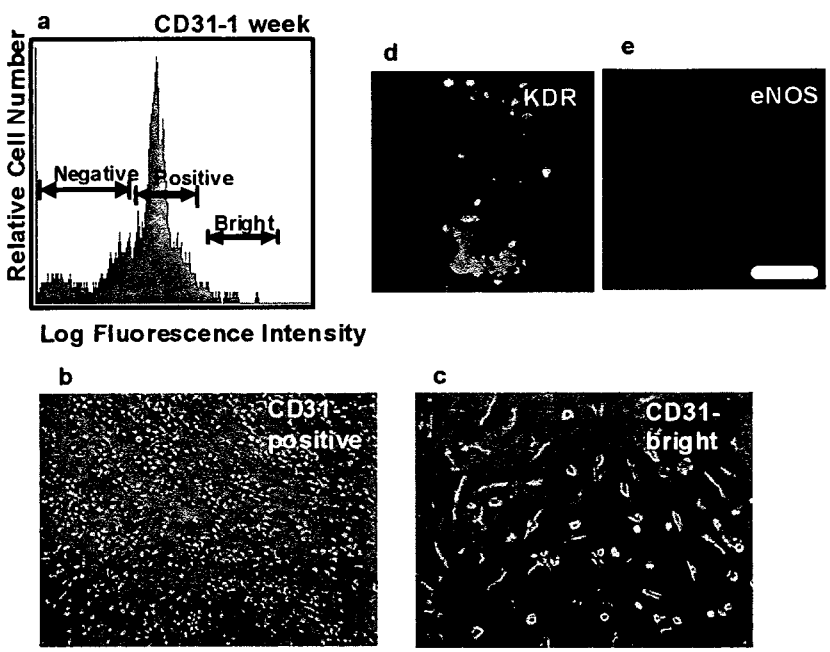

Fig.88 AC133陽性細胞から誘導したCD31強陽性early EPC

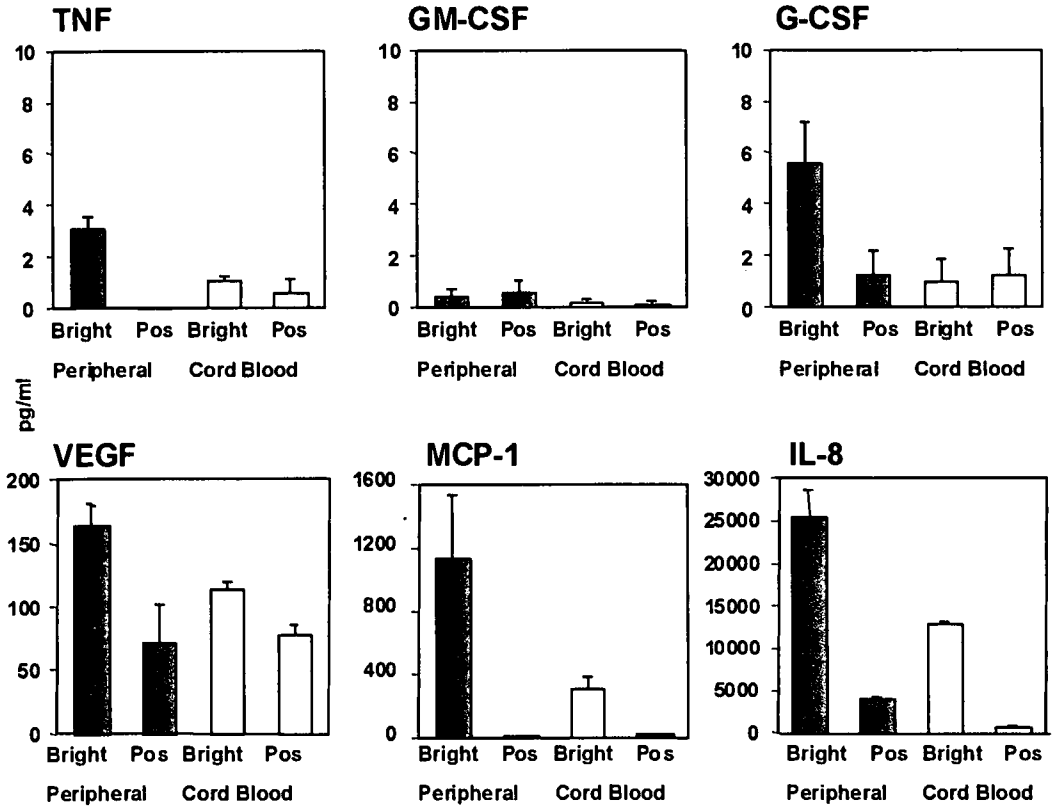

Fig. 89 AC133陽性細胞由来CD31陽性・強陽性細胞が放出するサイトカインの解析

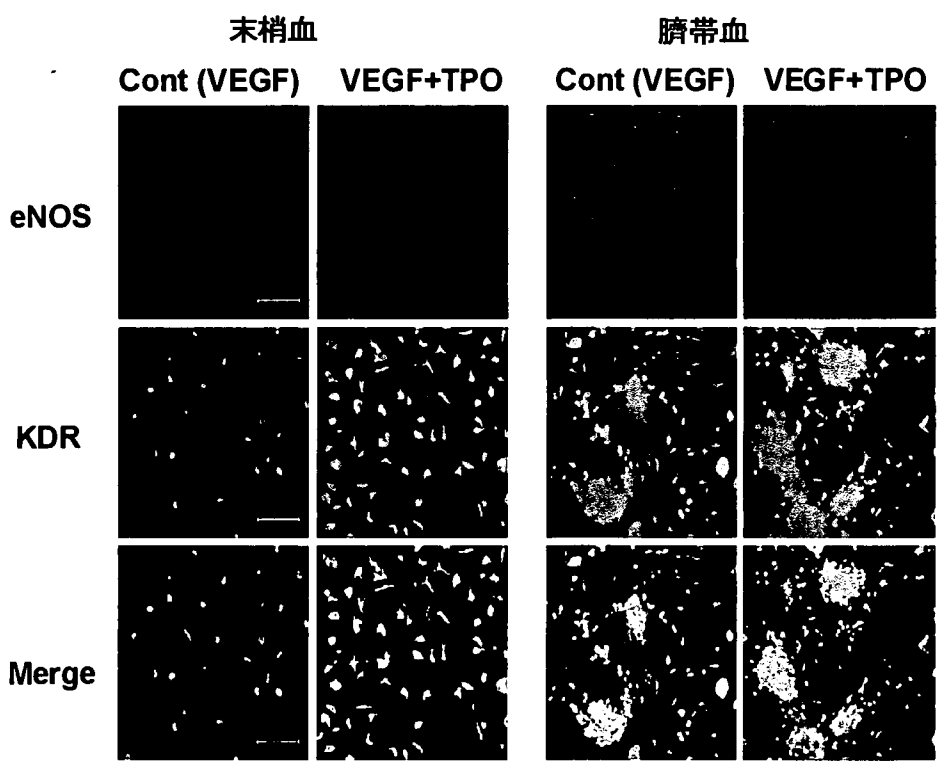

Fig. 90 TPOのEPC増幅作用

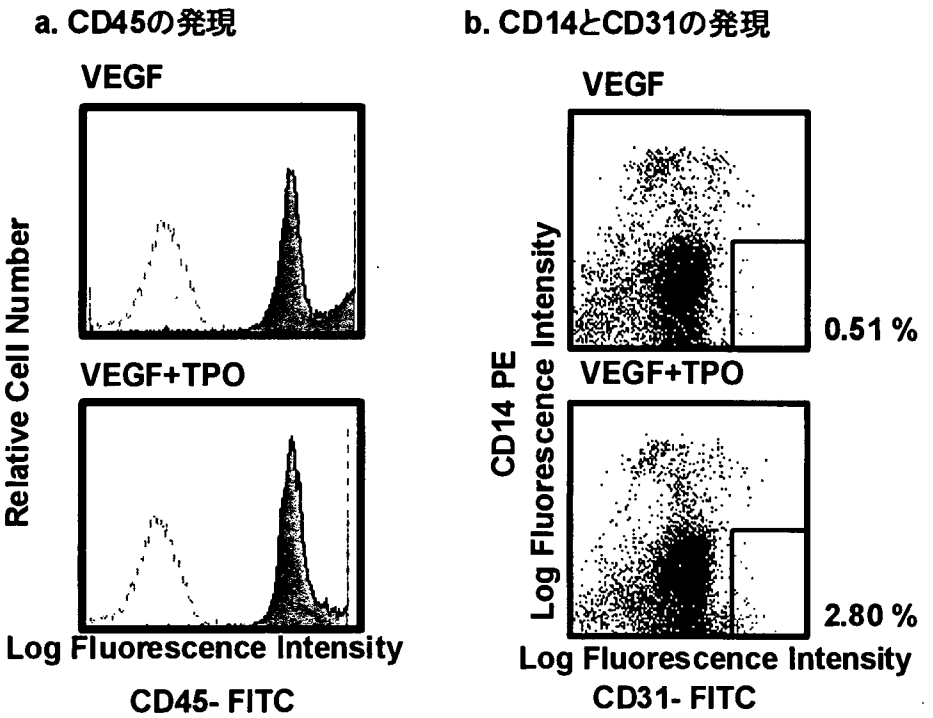

Fig. 91 培養AC133陽性細胞におけるCD45とCD14の発現

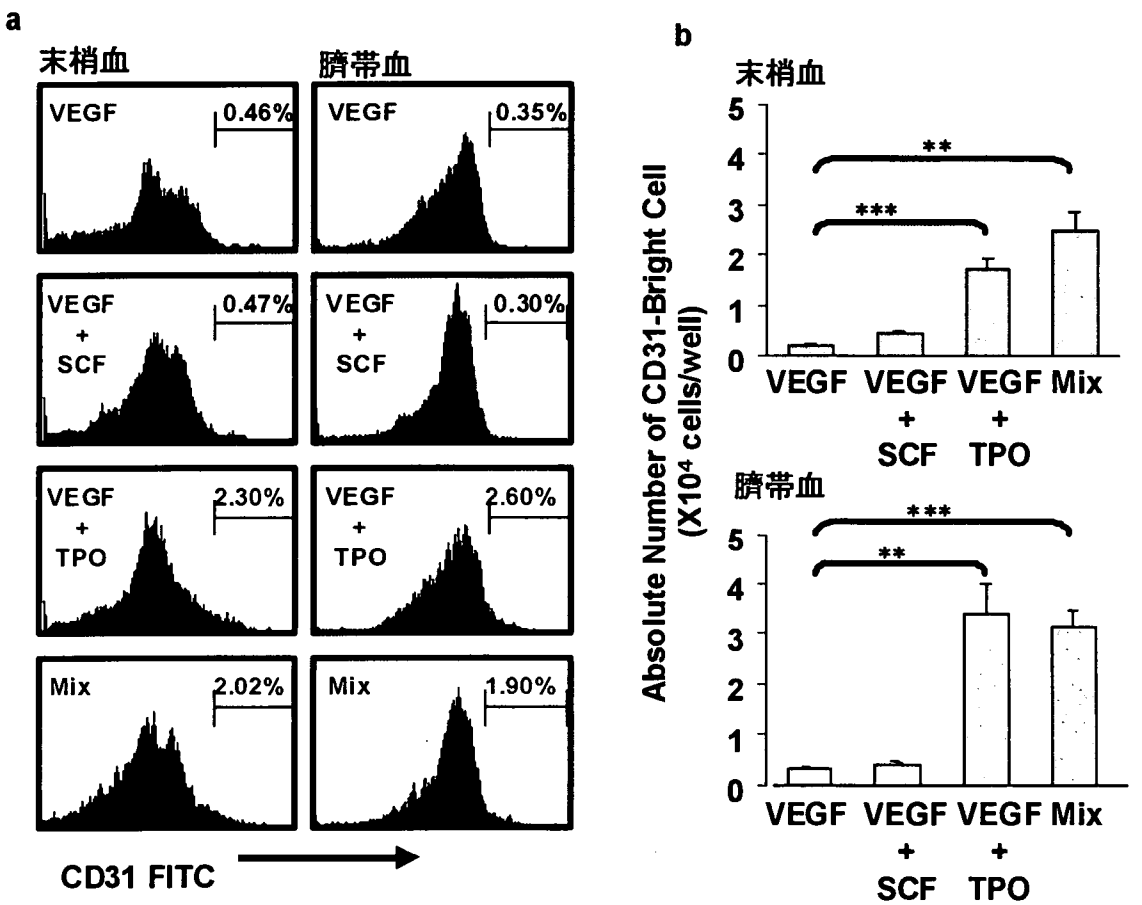

Fig. 92 CD31強陽性細胞出現に対するTPOの効果

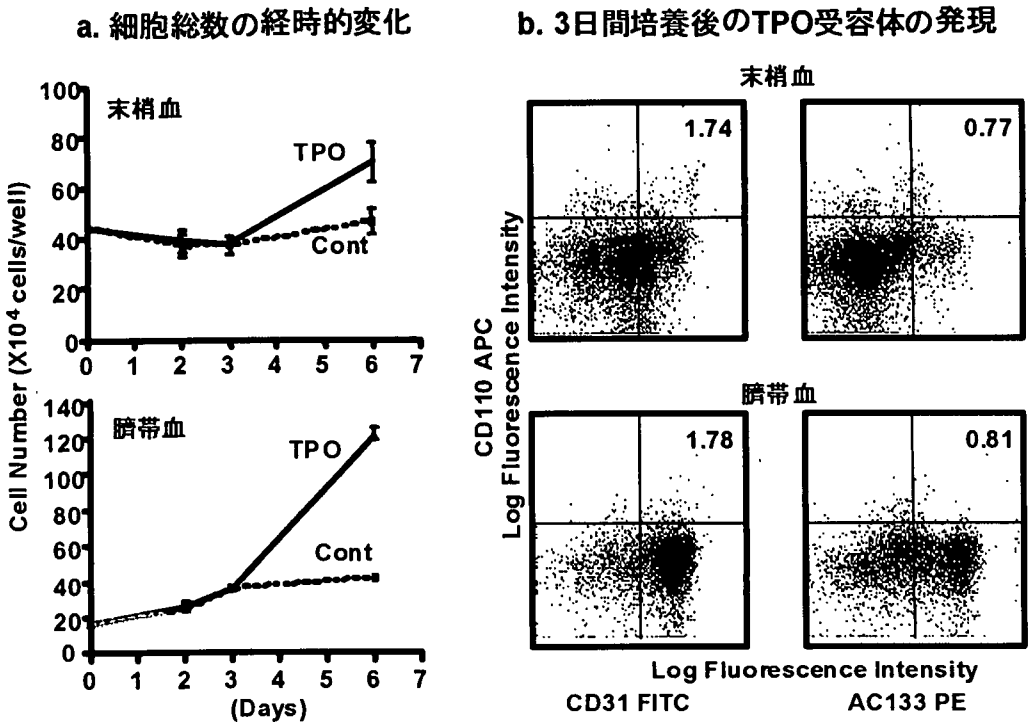

Fig. 93 AC133⁺細胞におけるTPO添加によるEPC増幅作用の経時変化

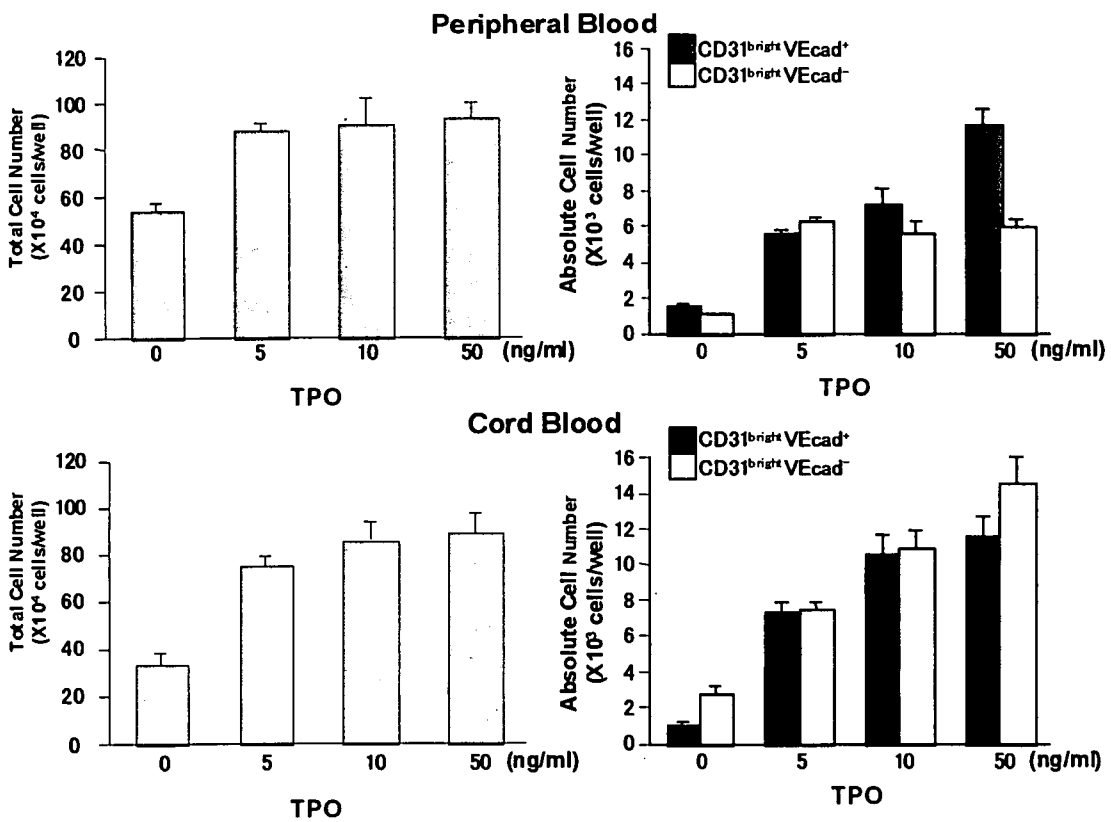

Fig. 94 CD31強陽性細胞出現に対するTPOの効果

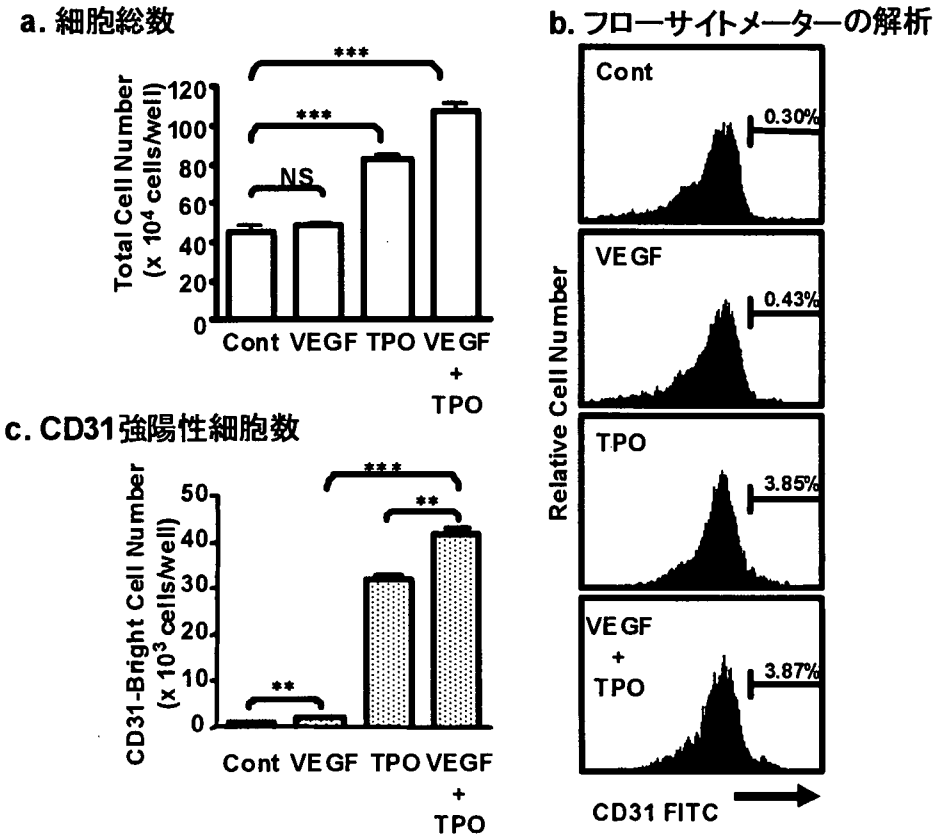

Fig. 95　EPC増幅作用におけるTPOとVEGFの比較

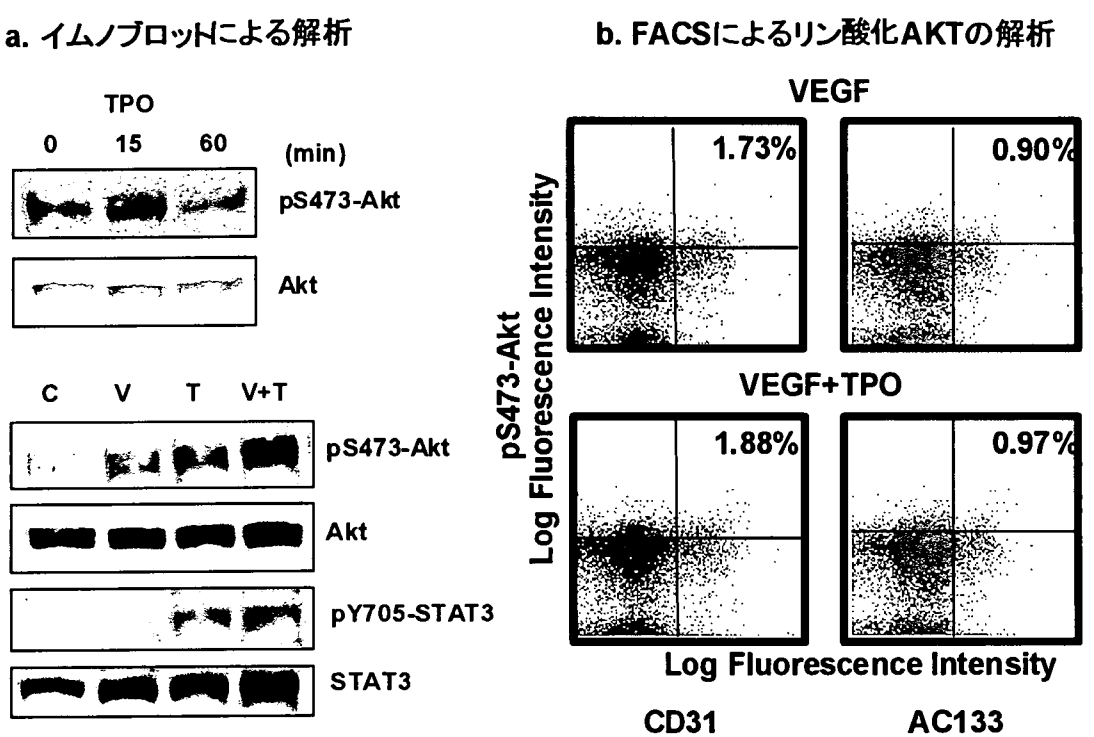

Fig. 96　AC133⁺細胞におけるTPO添加によるAKT及びSTAT3のリン酸化

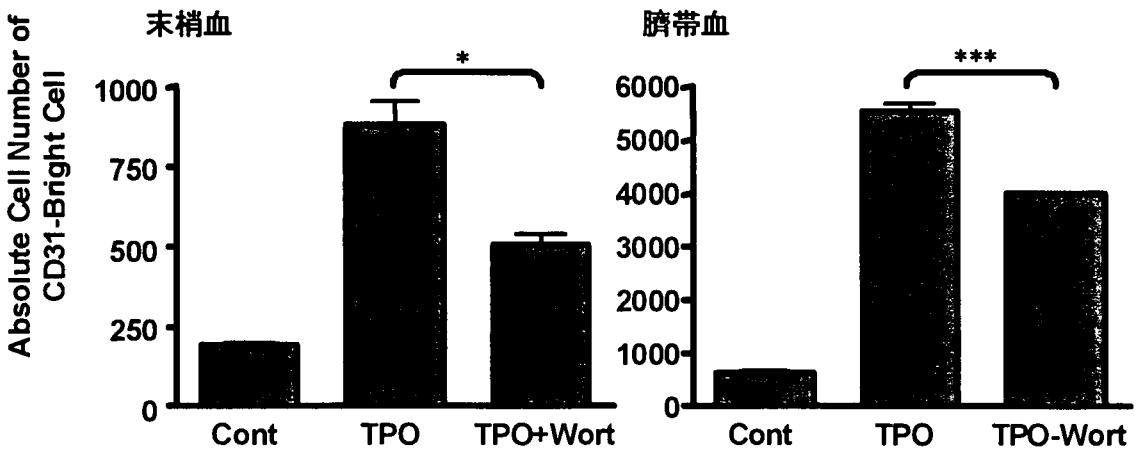

Fig. 97 TPOのEPCの分化・増殖作用におけるワートマニンの効果

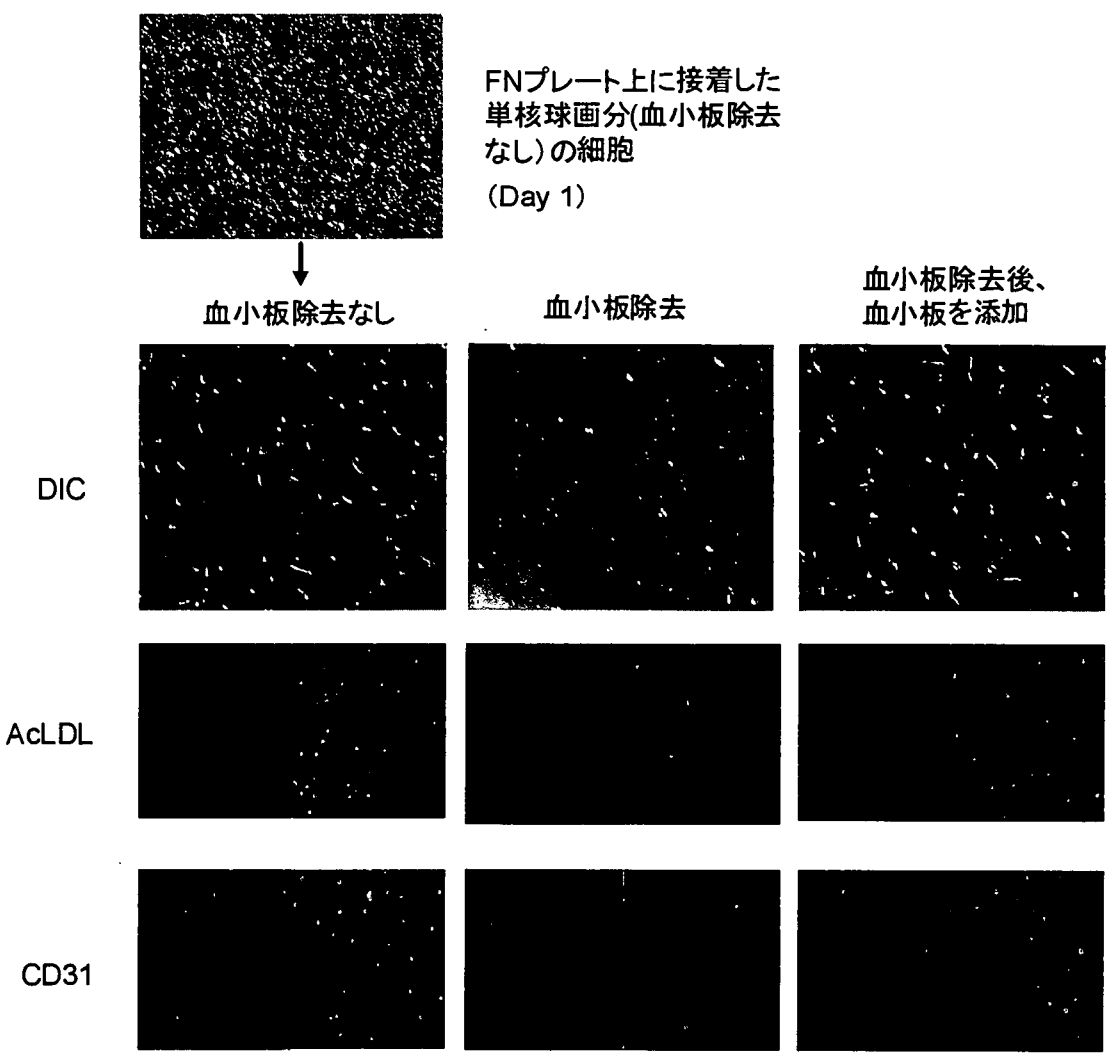

Fig. 98 単核球からのEarly EPC誘導に対する血小板の影響(Day6)